# Vibronic Spectroscopy with Submolecular Resolution from STM-Induced Electroluminescence

Benjamin Doppagne, Michael C. Chong, Etienne Lorchat, Stéphane Berciaud, Michelangelo Romeo, Hervé Bulou, Alex Boeglin, Fabrice Scheurer, and Guillaume Schull*

*Université de Strasbourg, CNRS, IPCMS, UMR 7504, F-67000 Strasbourg, France*

(Received 30 November 2016; published 21 March 2017)

A scanning tunneling microscope is used to generate the electroluminescence of phthalocyanine molecules deposited on NaCl/Ag(111). Photon spectra reveal an intense emission line at ≈1.9 eV that corresponds to the fluorescence of the molecules, and a series of weaker redshifted lines. Based on a comparison with Raman spectra acquired on macroscopic molecular crystals, these spectroscopic features can be associated with the vibrational modes of the molecules and provide a detailed chemical fingerprint of the probed species. Maps of the vibronic features reveal submolecularly resolved structures whose patterns are related to the symmetry of the probed vibrational modes.

DOI: 10.1103/PhysRevLett.118.127401

Near infrared [1], Raman [2], and low-temperature fluorescence [3] spectroscopies are powerful optical approaches to gather detailed chemical, structural, or environmental information on organic systems. Extremely sensitive to vibrational modes, it is considered that these techniques provide an unambiguous fingerprint of the probed species. Conversely, the scanning tunneling microscope (STM) enables imaging organic or inorganic objects with atomic resolution but lacks chemical sensitivity. Pechenezhskiy *et al.* recently developed an infrared STM able to detect the vibronic signature of monolayer assemblies of molecules [4]. This method, however, could not yet reach single-molecule sensitivity. Nearly at the same time, Zhang *et al.* made an important step towards combining the chemical sensitivity of Raman spectroscopy with the spatial resolution of STM [5]. They performed tip-enhanced Raman spectroscopy (TERS) of molecules with subnanometric resolution using the tip of a STM as a plasmonic antenna to amplify a laser excitation.

Because they can be confined to atomic-scale pathways, we propose here to use electrons rather than photons as an excitation source of the vibronic signal. This approach is based on our observation of vibronic peaks in the low-temperature fluorescence spectra of a single molecule excited by STM [6,7]. A comparison to calculated vibrational spectra led us to suggest that these peaks correspond to the different molecular vibration modes, in contrast to earlier STM-induced light emission (STM-LE) experiments where similar features pertained to the harmonic progression of a single mode [8–12]. However, because of the low intensity of the signal and the lack of comparable spectroscopic data for this molecule in the literature, a definitive conclusion regarding the nature of the vibronic features could not be reached. Moreover, in this experiment, the molecular emitter is suspended in the STM junction, and the spatial resolution of the STM is lost.

Here we demonstrate that spatial resolution and detailed vibronic spectroscopy can be combined in a single experiment without an optical excitation. Following an approach reported recently [13–15], we address the optoelectronic properties of zinc-phthalocyanine (ZnPc) molecules decoupled from a Ag(111) surface by a thin insulating layer of salt (NaCl). STM-LE spectra of these molecules reveal a sharp and intense emission line around 1.9 eV which corresponds to the fluorescence of ZnPc. Our spectra also show several weaker emission lines at lower energy. Extremely well reproduced by Raman spectra acquired on bulk ZnPc aggregates and fluorescence measurements on ZnPc trapped in frozen matrices [16], these emission lines are associated to the vibrational modes of the molecule and constitute an accurate spectroscopic fingerprint of the probed species [17]. Submolecular spatial variations of the vibronic peak intensities were observed by scanning the molecule with the STM tip. In contrast to resonant TERS maps [5] that are insensitive to the probed vibronic mode [18], the patterns in our STM-LE vibronic maps reflect the symmetry of the considered modes [19], an effect that is interpreted in the framework of vibronic coupling theory [20].

The STM data were acquired with a low temperature (4.5 K) Omicron setup operating in ultrahigh vacuum adapted to detect the light emitted at the tip-sample junction. The optical detection setup is composed of a spectrograph coupled to a CCD camera and provides a spectral resolution of ≈0.8 nm. The details of the optical setup are described in the Supplemental Material of Ref. [6]. Tungsten STM tips were introduced in the sample to cover them with silver and to tune their plasmonic response. The Ag(111) substrates were cleaned with successive sputtering and annealing cycles. Approximately 0.5 monolayer of NaCl was sublimed on Ag(111) kept at room temperature, forming square bi- and

 

trilayers. Eventually, ZnPc molecules were evaporated on the cold NaCl/Ag(111) sample in the STM chamber. DFT calculations of single ZnPc molecules were carried out at the B3LYP/6-13G level in the full $D4h$ geometry to determine the vibrational modes and their symmetries [21]. The calculated vibrational frequencies were scaled by 0.9613 as recommended [22].

Figure 1(a) is an illustration of the experiment where an STM tip is used to excite the luminescence of ZnPc adsorbed on a 2ML-NaCl/Ag(111) substrate. Figure 1(b) is an STM image of a single molecule, a dimer and a tetramer of ZnPC assembled on this surface. The molecular arrangements are formed by STM-tip manipulation following the procedure established in Ref. [13]. The optical spectrum in Fig. 1(c) is obtained by locating the STM-tip on the extremity of the tetramer [arrow in Fig. 1(b)] and applying a sample voltage of $V = -2.5$ V with a current setpoint $I = 0.75$ nA. The electroluminescence spectrum shows an intense emission line at 663 nm—the 0-0 transition—and several redshifted peaks of lower intensity (magnified by 50 in the top part of the panel). The main line is assigned to the emission of an excitonic state delocalized over several molecules [13]. The weaker lines (not reported in Ref. [13]) are represented as a function of their energy shift from the 0-0 line chosen as origin of the abscissa. They are compared in Fig. 1(c) to an experimental Raman spectrum of a bulk ZnPc crystal acquired for close-to-resonance excitation. The number, the energies and the relative intensities of the different peaks are nearly identical in these two spectra. These data are also in excellent agreement with photoluminescence spectra acquired on ZnPc molecules isolated in cryogenic matrices [16]. Based on a comparison with DFT calculations, the emission lines can be precisely assigned to distinct vibrational modes of the ZnPc molecule [Fig. 1(d)]. Our STM-LE spectra therefore constitute a chemical fingerprint of the probed species.

Figure 2(b) shows the STM-LE spectra recorded for linear arrangements of 1 to 4 ZnPc molecules [Fig. 2(a)]. The 0-0 peak sharpens and shifts to lower energies with the number of molecules in the chain. These effects are the consequence of the coherent coupling of the molecular dipoles [13]. While the vibronic peaks appear at different wavelengths [Fig. 2(c)] depending on the length of the linear arrangement, Fig. 2(d) reveals an invariant energy shift of the vibronic modes with respect to the 0-0 line. Moreover, the widths of the vibronic peaks decrease when the number of molecules in the chain increases, following the same trend observed for the 0-0 line. These observations suggest that the 0-0 and the vibronic emissions correspond to radiative transitions that originate from the same excited state of the molecules.

We now focus on the spatial dependency of the vibronic signal. Figure 3(a) shows 3 spectra acquired for different locations of the STM tip on a molecular trimer [square, dot, and star marks in Fig. 3(b)]. The intensity of the 0-0 line varies substantially as a function of the tip location. This effect has been described in details in Ref. [13] and is another manifestation of the coupling between the

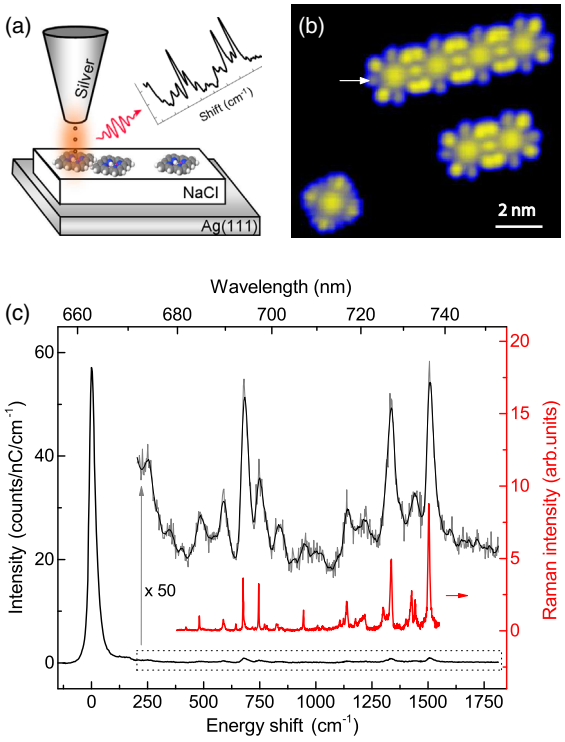


(d)

| STM-LE | Raman | Ar matrix | DFT | |
|---|---|---|---|---|
| 475 | 474 | 490 | 471 | $B_{2g}$ |
| 579 | 580 | 598 | 579 | $A_{1g}$ |
| 679 | 669 | 689 | 664 | $A_{1g}$ |
| 752 | 738 | 751 | 734 | $B_{1g}$ |
| 837 | 817 | 845 | 823 | $B_{1g}$ |
| 942 | 938 | 945 | 923 | $B_{2g}$ |
| 1144 | 1130 | 1150 | 1165 | $B_{1g}$ |
| 1209 | 1210 | 1221 | 1195 | $B_{2g}$ |
| 1335 | 1330 | 1346 | 1333 | $A_{1g}$ |
| 1438 | 1420<br>1435 | 1448 | 1429 | $B_{1g}$ |
| 1509 | 1497 | 1525 | 1528 | $B_{1g}$ |

FIG. 1. (a) Sketch of the STM-induced emission experiment. (b) STM image ($I = 30$ pA, $V = -2.5$ V) of a single ZnPc molecule (lower left), a dimer (lower right) and a linear tetramer (top right) of ZnPc molecules deposited on NaCl/Ag(111). (c) STM-induced light emission spectrum (black line) of the ZnPc linear tetramer [$I = 0.75$ nA, $V = -2.5$ V, $t = 300$ s, tip located at the white arrow in (b)]. The right part of the spectrum is represented magnified by 50 and compared to a resonance Raman spectra acquired on a ZnPc crystal at room temperature and in air (excitation wavelength 632.8 nm). The raw (smoothed) data appear in gray (black) in the magnified spectrum. (d) Frequency shifts (in $cm^{-1}$) of the vibronic peaks in the STM-LE and Raman spectra displayed in (c), in the fluorescence spectra of ZnPc molecules trapped in frozen Argon matrices taken from Ref. [16] and assignment to vibrational modes of the ZnPc with their respective symmetry based on DFT calculations.

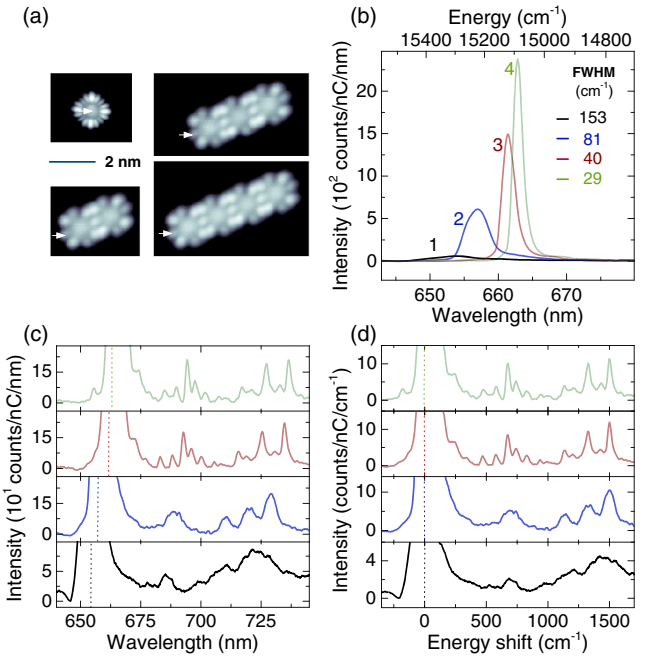


FIG. 2. (a) STM images ($I = 30$ pA, $V = -2.5$ V) and (b) STM-LE spectra acquired for a single molecule, a dimer, a trimer and a tetramer of molecules deposited on NaCl/Ag(111) ($V = -2.5$ V). The white arrows in (a) mark the location of the tip during the acquisition of the optical spectra. The peak width in the case of the tetramer is only 60% larger than our spectral resolution; consequently its FWHM is slightly overestimated. The panels (c) and (d) show the low energy vibrational features of the same spectra as a function of the wavelength (c) and as a function of the shift from the 0-0 lines (d).

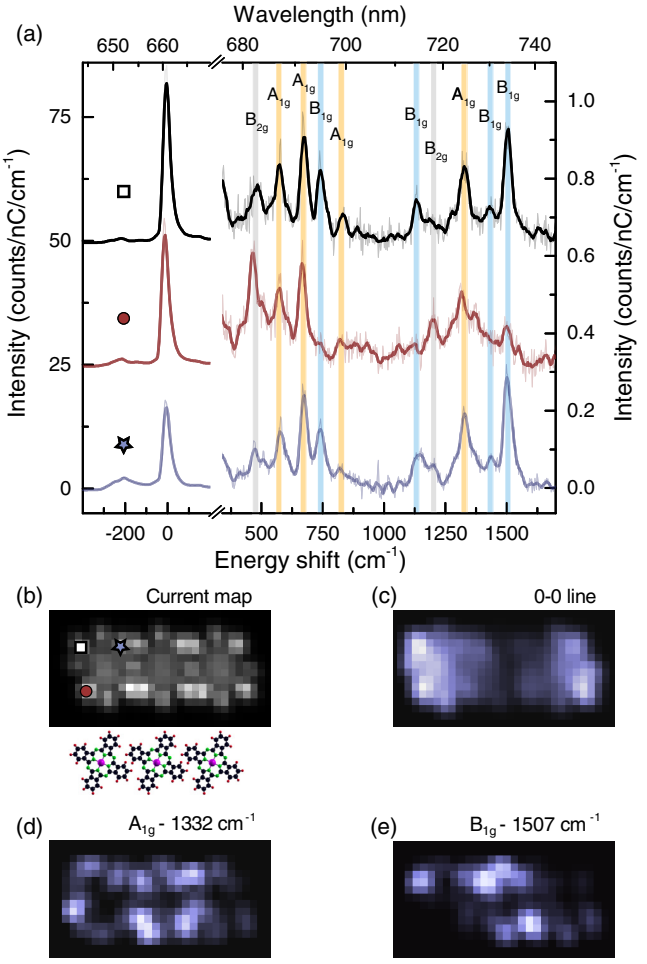


FIG. 3. (a) STM-induced light emission spectra ($V = -2.5$ V) acquired for three positions of the tip [coloured marks in (b)] with respect to a molecular trimer. The spectra are vertically shifted for clarity. (b) Constant height STM image of the trimer ($5.1 \times 2.7$ nm$^2$, $V = -2.5$ V) and its scaled model. Normalized photon intensity maps for (c) the 0-0 emission and for (d) the 1332 and (e) 1507 cm$^{-1}$ peaks ($5.1 \times 2.7$ nm$^2$, $V = -2.5$ V, time/pixel = 10 s. The photon maps were slightly processed with a Gaussian smoothing algorithm.)

molecular dipoles. The number and the energy of the vibronic peaks do not change, but the intensities of some peaks vary depending on the tip position. Here, three different behaviors can be distinguished: In a first group, the (yellow) peaks show an almost constant intensity in the three spectra. In a second group, the (blue) peaks are intense in the top and bottom spectra and strongly attenuated in the middle spectrum. In a third group, the (gray) peaks show the opposite pattern, with a low intensity in the top and bottom spectra and a high intensity in the middle spectrum. No obvious correlation with the intensity variation of the 0-0 line is observed, suggesting that the intensities of the vibronic peaks are weakly affected by the efficiency of the optical transition resulting in the 0-0 line. In the top panel, we indicate the irreducible representation of each mode as deduced by DFT calculations and comparison with earlier works [16,22]. The three families of peaks are related to well-defined irreducible representations of ZnPc. The peaks having a constant intensity stem from ZnPc modes having $A_{1g}$ symmetry, while the second and third groups stem from ZnPc modes of $B_{1g}$ and $B_{2g}$ representations, respectively. To get further insight into this phenomenon, we recorded maps of the light intensity [10,13,23–25] at the energy of the 0-0 line [Fig. 3(c)], for a vibronic peak whose intensity remains constant with tip position [$h\nu = 1332$ cm$^{-1}$; $A_{1g}$; Fig. 3(d)] and for a peak whose intensity varies [$h\nu = 1507$ cm$^{-1}$; $B_{1g}$; Fig. 3(e)]. These maps were acquired with a constant tip-sample distance (open feedback loop) in order to prevent possible artifacts due to the tip trajectory. At each pixel, an emission spectrum is recorded. A background is then subtracted to remove the contribution of the plasmonic emission. The spectra are eventually normalized by the tunneling current measured during the acquisition to correct for the higher (lower) excitation rate at high (low) current. The photon map at the energy of the 0-0 line [Fig. 3(c)] shows two maxima at the extremities of the trimer, a behavior that is attributed to the coherent coupling between the molecular dipoles [13]. This map is remarkably

different from those acquired at the energy of the vibronic peaks [Figs. 3(d), 3(e)], confirming that the spatial dependencies of the vibronic peak intensities are not correlated to that of the 0-0 transition. Interestingly, the pattern in the vibronic photon maps is of higher symmetry for the mode at 1332 $cm^{-1}$ than for the mode at 1507 $cm^{-1}$, reflecting the higher symmetry of $A_{1g}$ compared to $B_{1g}$ modes.

In the following we provide an interpretation for the patterns in the photon maps. In Fig. 2, a close relationship between the position and the width of the 0-0 line and the vibronic peaks is evidenced while Fig. 3 reveals an independent spatial variation of their intensities. These aspects may be reconciled assuming an interpretation of the spectral features in the frame of molecular vibronic coupling theory [20]. Indeed, in a purely Franck and Condon (FC) picture, one would expect the maps acquired at the energy of the vibronic peaks [Figs. 3(d),(e)] to all faithfully reproduce the one of the 0-0 transition since all the lines in the spectrum stem from the same electronic transition and only their relative intensities are proportional to vibrational wave function overlap integrals (whose squares are the FC factors). A similar argumentation was developed [18] to explain the strong resemblance between TERS maps acquired on a single molecule for different vibronic modes [5]. The spatial dependency of the vibronic peaks in Fig. 3 suggests that we need to move beyond the FC picture and to consider that the vibrational emission is provided by Herzberg-Teller contributions (i.e., the simultaneous change in electronic and vibrational states not due to simple vibrational overlaps). Here, the vibronic transitions directly depend on the admixture of electronic states of high energy that contribute to the lowest energy transition. This coupling directly depends on the vibrational mode considered, thus providing the relation between mode symmetry and the map patterns in Fig. 3. A more detailed discussion of this mechanism is provided in Supplemental Material [26].

Having formulated a tentative rationalization of the experimental observations, we now discuss the excitation mechanism. STM-induced fluorescence of single-molecules has been reported in an increasing number of cases [6–15,28]. In most of them (including Ref. [13] on the same system) it was concluded that the luminescence involves a diodelike behavior [Fig. 4(a)] where electrons and holes injected in the molecule from the electrodes recombine and produce a photon. In this model, the frontier orbitals shift with voltage with respect to the Fermi levels of the tip and sample. Such a scenario happens when the voltage drop between the molecule and the surface ($Vd_S$) is of the same magnitude than between the molecule and the tip ($Vd_T$). However, conductance spectra acquired as a function of the tip-molecule distance show no shift of the frontier orbitals of the molecule [Fig. 4(c)], a behavior indicating that the voltage drops nearly exclusively on one side of the molecule (the tip side according to similar experiments [29]). This

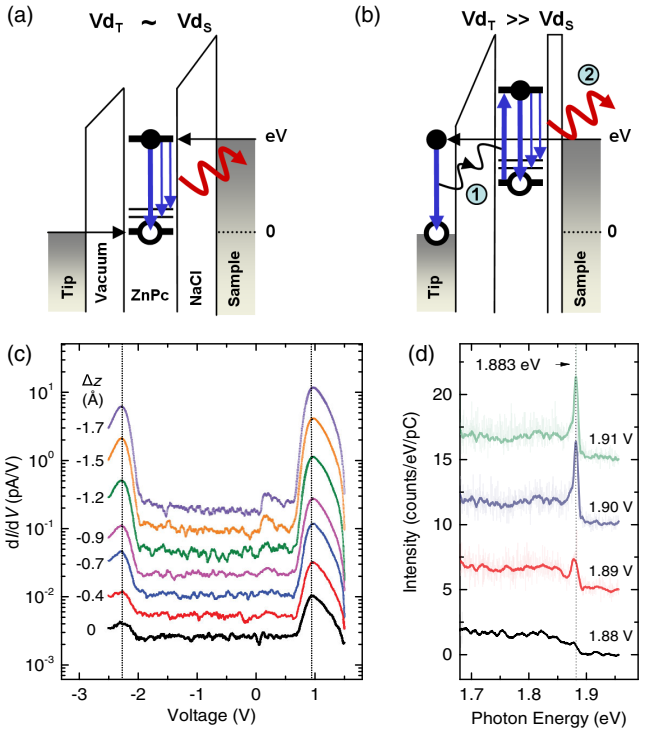


FIG. 4. Sketches (a) of the diodelike emission mechanism and (b) of the energy transfer mechanism. (c) $dI/dV$ spectra (in log scale) acquired on a molecular dimer for different tip-molecule distances $\Delta z$. $\Delta z = 0$ corresponds to a current set point of $I = 7.5$ pA at $V = -2.5$ V. (d) Light spectra acquired on the same dimer as a function of voltage ($I = 150$ pA, $t = 180$ s). The spectra are vertically shifted for clarity.

configuration is therefore not compatible with a diodelike mechanism involving a rigid shift of the molecular orbitals with voltage. In contrast, the spectra in Fig. 4(d) show that the voltage onset of the 0-0 line exactly matches the energy of the 0-0 transition. This rather suggests an energy transfer [Fig. 4(b)] between the tunneling electrons and the molecule ① mediated by the plasmons localized at the tip-sample junction. The excited molecule then relaxes to the ground or to an excited vibrational state of the electronic ground state by emitting a photon ②. A similar interpretation was first proposed to explain the luminescence spectra of large molecular aggregates [30,31] and the emission of single molecules suspended in a STM junction [6,7]. This mechanism was nicely confirmed for single molecules adsorbed flat on an insulating layer [15].

In conclusion, our experiment provides a way to obtain a high chemical sensitivity with sub-molecular scale spatial resolution without resorting to an optical excitation. By using electrons rather than photons to excite the low-temperature fluorescence of ZnPc molecules, vibronic signals with submolecular resolution were obtained. This approach could be extended to any fluorescent molecule emitting in the visible and should allow distinguishing different chromophores coadsorbed on a same surface. In

contrast to resonant TERS maps [5] that are insensitive to the vibronic modes [18], the patterns of our STM-LE "vibronic maps" are intimately linked to the mode symmetry. This is rationalized by considering the different origin of the vibronic emission in these two experiments. While the resonant TERS signals finds its origin in the dominant character of the Franck-Condon term, Herzberg-Teller contributions prevail in our spectra. We envision that performing the two approaches on the very same system would help to better understand the origin of this difference. Our approach therefore constitutes a decisive step towards a vibronic mode spectroscopy of molecules with subnanometric resolution.

The authors thank Jean-Louis Gallani for the absorption and fluorescence spectra of the ZnPc molecules in solution and Virginie Speisser, Jean-Georges Faullumel, and Olivier Cregut for technical support. The Agence Nationale de la Recherche (project SMALL'LED No. ANR-14-CE26-0016-01), the Labex NIE (Contract No. ANR-11-LABX-0058_NIE), the Equipex UNION (Contract No. ANR-10-EQPX-52-01), the Région Alsace and the International Center for Frontier Research in Chemistry (FRC) are acknowledged for financial support.

*guillaume.schull@ipcms.unistra.fr

[1] M. Blanco and I. Villarroya, Trends Anal. Chem. **21**, 240 (2002).
[2] D. J. Gardiner and P. R. Graves, *Practical Raman Spectroscopy* (Springer-Verlag, New York, 1989).
[3] A. V. Naumov, Phys. Usp. **56**, 605 (2013).
[4] I. V. Pechenezhskiy, X. Hong, G. D. Nguyen, J. E. P. Dahl, R. M. K. Carlson, F. Wang, and M. F. Crommie, Phys. Rev. Lett. **111**, 126101 (2013).
[5] R. Zhang, Y. Zhang, Z. C. Dong, S. Jiang, C. Zhang, L. G. Chen, L. Zhang, Y. Liao, J. Aizpurua, Y. Luo, J. L. Yang, and J. G. Hou, Nature (London) **498**, 82 (2013).
[6] M. C. Chong, G. Reecht, H. Bulou, A. Boeglin, F. Scheurer, F. Mathevet, and G. Schull, Phys. Rev. Lett. **116**, 036802 (2016).
[7] M. C. Chong, L. Sosa-Vargas, H. Bulou, A. Boeglin, F. Scheurer, F. Mathevet, and G. Schull, Nano Lett. **16**, 6480 (2016).
[8] X. H. Qiu, G. V. Nazin, and W. Ho, Science **299**, 542 (2003).
[9] S. W. Wu, G. V. Nazin, and W. Ho, Phys. Rev. B **77**, 205430 (2008).
[10] C. Chen, P. Chu, C. A. Bobisch, D. L. Mills, and W. Ho, Phys. Rev. Lett. **105**, 217402 (2010).
[11] S.-E. Zhu, Y.-M. Kuang, F. Geng, J.-Z. Zhu, C.-Z. Wang, Y.-J. Yu, Y. Luo, Y. Xiao, K.-Q. Liu, Q.-S. Meng, L. Zhang, S. Jiang, Y. Zhang, G.-W. Wang, Z.-C. Dong, and J. G. Hou, J. Am. Chem. Soc. **135**, 15794 (2013).
[12] J. Lee, S. M. Perdue, A. Rodriguez Perez, and V. A. Apkarian, ACS Nano **8**, 54 (2014).
[13] Y. Zhang, Y. Luo, Y. Zhang, Y.-J. Yu, Y.-M. Kuang, L. Zhang, Q.-S. Meng, Y. Luo, J.-L. Yang, Z.-C. Dong, and J. G. Hou, Nature (London) **531**, 623 (2016).
[14] H. Imada, K. Miwa, M. Imai-Imada, S. Kawahara, K. Kimura, and Y. Kim, Nature (London) **538**, 364 (2016).
[15] H. Imada, K. Miwa, M. Imai-Imada, S. Kawahara, K. Kimura, and Y. Kim, arXiv:1609.02701.
[16] C. Murray, N. Dozova, J. G. McCaffrey, N. Shafizadeh, W. Chin, M. Broquier, and C. Crepin, Phys. Chem. Chem. Phys. **13**, 17543 (2011).
[17] E. Cavar, M.-C. Blüm, M. Pivetta, F. Patthey, M. Chergui, and W-D. Schneider, Phys. Rev. Lett. **95**, 196102 (2005).
[18] S. Duan, G. Tian, Y. Ji, J. Shao, Z. Dong, and Y. Luo, J. Am. Chem. Soc. **137**, 9515 (2015).
[19] N. Pavliček, I. Swart, J. Niedenführ, G. Meyer, and J. Repp, Phys. Rev. Lett. **110**, 136101 (2013).
[20] G. Fisher, *Vibronic Coupling: The Interaction between the Electronic and Nuclear Motions* (Academic Press, London, 1984).
[21] GAUSSIAN 09, Revision B.01, Gaussian Inc., Wallingford CT (USA), 2010.
[22] Z. Liu, X. Zhang, Y. Zhang, and J. Jiang, Spectrochim. Acta A **67**, 1232 (2007).
[23] R. Berndt and J. K. Gimzewski, Surf. Sci. **269–270**, 556 (1992).
[24] G. Schull, M. Becker, and R. Berndt, Phys. Rev. Lett. **101**, 136801 (2008).
[25] C. Große, O. Gunnarsson, P. Merino, K. Kuhnke, and K. Kern, Nano Lett. **16**, 2084 (2016).
[26] See Supplemental Material at http://link.aps.org/supplemental/10.1103/PhysRevLett.118.127401, which include Ref. [27], for details regarding the theoretical framework of the proposed interpretation.
[27] T. Azumi and K. Matsuzaki, Photochem. Photobiol. **25**, 315 (1977).
[28] G. Reecht, F. Scheurer, V. Speisser, Y. J. Dappe, F. Mathevet, and G. Schull, Phys. Rev. Lett. **112**, 047403 (2014).
[29] J. Repp, G. Meyer, S. M. Stojković, A. Gourdon, and C. Joachim, Phys. Rev. Lett. **94**, 026803 (2005).
[30] Z. C. Dong, X. L. Zhang, H. Y. Gao, Y. Luo, C. Zhang, L. G. Chen, R. Zhang, X. T. Y. Zhang, J. L. Yang, and J. G. Hou, Nat. Photonics **4**, 50 (2010).
[31] N. L. Schneider and R. Berndt, Phys. Rev. B **86**, 035445 (2012).